International Immunopharmacology 70 (2019) 324–337

Contents lists available at ScienceDirect

International Immunopharmacology

journal homepage: www.elsevier.com/locate/intimp

Doxycycline hyclate: A schistosomicidal agent *in vitro* with immunomodulatory potential on granulomatous inflammation *in vivo*

Miriam Viviane Dias[a], Aline Pereira Castro[c], Camila Cabral Campos[a], Thaiany Goulart Souza-Silva[a], Reggiani Vilela Gonçalves[d], Raquel Lopes Martins Souza[b], Marcos José Marques[b], Rômulo Dias Novaes[a,*]

[a] Institute of Biomedical Sciences, Department of Structural Biology, Federal University of Alfenas, Alfenas, Minas Gerais, Brazil
[b] Institute of Biomedical Sciences, Department of Pathology and Parasitology, Federal University of Alfenas, Alfenas, Minas Gerais, Brazil
[c] Faculty of Pharmaceutical Sciences, Federal University of Alfenas, Alfenas, Minas Gerais, Brazil
[d] Department of Animal Biology, Federal University of Viçosa, Viçosa, Minas Gerais, Brazil

ARTICLE INFO

Keywords:
Antiparasitic chemotherapy
Experimental pathology
Parasitology
Schistosomiasis

ABSTRACT

We investigated the effect *in vitro* and *in vivo* of doxycycline hyclate (Dx), a broad-spectrum antibiotic inhibitor of matrix metaloproteinases (MMPs), on adult *Schistosoma mansoni* worms and granulomatous liver inflammation in infected mice. Adult *S. mansoni* worms in culture treated with different concentrations of Dx (50–180 μg/mL) were studied for eight days to assess its morphology, eggs production, and mortality. Uninfected mice and those infected with *S. mansoni*, untreated and treated with praziquantel (Pz; 200 mg/kg) or Dx (50 mg/kg), were evaluated for 60 days. Our results indicated that Dx induced dose-dependent integumentary lesions (bubbles, tubercle collapse, spicule disappearance, peeling, and erosion), reduced mating rate and eggs-laying in adult *S. mansoni* worms. The effective lethal dose required to kill 50% of worms was 112.0 μg/mL Dx (DL_{50}). In mice, *S. mansoni* infection induced hepatomegaly, intense IL-4, IL-10, TNF-α and TGF-β production, granulomatous inflammation and hepatic glycogen depletion. The number and size of the granulomas was similar in untreated and Dx-treated animals. Untreated animals showed a predominance of productive granulomas, and intense MMP-2 and MMP-9 activities. Dx-treated mice exhibited a significant increase in IL-4 levels, tissue inflammation, proportion of involutive granulomas, and hepatic collagenogenesis, as well as attenuated MMP-2 and MMP-9 activities. Our findings indicated that Dx is toxic to adult *S. mansoni* worms *in vitro*. However, *in vitro* beneficial effects were not reproduced *in vivo*, since Dx treatment increased liver granulomatous inflammation and collagenogenesis in *S. mansoni*-infected mice by a process potentially associated with Dx-mediated hepatic MMP-2 and MMP-9 inhibition.

1. Introduction

Schistosomiasis is a disease caused by trematodes of the genus Schistosoma [1,2]. Considering all *Schistosoma* species, about 240 million people in 78 countries are infected and 800 million people live in areas endemic to the disease. In the world, the highest incidence and prevalence of schistosomiasis occurs in regions of the Middle East, South America, Southwest Asia and especially Africa [3,4]. The species responsible for schistosomiasis in Brazil is *Schistosoma mansoni*, which causes a chronic and debilitating disease [4]. In this country, about 25 million people live in an area with a risk of schistosomiasis and approximately 2.5 to 6 million individuals are infected, especially in poor and rural areas where sanitation and quality of life are precarious [5,6].

The life cycle of *S. mansoni* is heteroxenic, passing one phase in the mollusk, the intermediate host, and another phase in humans, the definitive hosts [7,8]. Schistosomiasis develops in humans in acute and chronic phases [9]. The acute phase is generally asymptomatic and represents a mild form with hepatointestinal involvement. The chronic phase, when symptomatic, manifests as hepatosplenomegaly and portal hypertension and is recognized as an advanced hepatosplenic form [10]. Acute schistosomiasis is characterized by the presence of numerous periovular granulomas in multiple organs, especially in the liver, intestines and lungs [10]. These granulomas are large, with a predominantly exudative component rich in eosinophils, poorly

* Corresponding author at: Institute of Biomedical Sciences, Department of Structural Biology, Federal University of Alfenas, Rua Gabriel Monteiro da Silva, 700, Alfenas 37130-001, Minas Gerais, Brazil.
E-mail address: romulo.novaes@unifal-mg.edu.br (R.D. Novaes).

https://doi.org/10.1016/j.intimp.2019.02.032
Received 29 January 2019; Received in revised form 13 February 2019; Accepted 19 February 2019
Available online 07 March 2019

delimited periphery and frequent periovular necrosis [11]. At the beginning of the chronic phase, granulomas are observed at various stages of evolution, including involutive forms with low cellularity and high collagen density [10]. During this phase, the arrival of new viable *S. mansoni* eggs in the tissues triggers concomitant granulomatous reactions similar to those observed in the acute phase [12,13]. In general, schistosomiasis granulomas are smaller in the chronic phase, since the inflammatory reaction is counterbalanced by the destruction of older granulomas [12]. The most advanced chronic phase is severe, being predominantly characterized by periportal hepatic fibrosis (Amral et al., 2017, [14]).

In general, fibrosis is the result of imbalance in the normal process of synthesis and degradation of extracellular matrix components, especially collagen [15]. Takahashi et al. [16] demonstrated that increased collagen production occurs parallel to collagenase synthesis in the liver during early-stage *S. mansoni* infection. According to Madala et al. [17], fibrosis results from the imbalance between collagen synthesis by interstitial cells and enzymatic degradation, especially by matrix metalloproteinases (MMPs). Matrix metalloproteinases play an essential role in extracellular matrix (ECM) remodeling by degrading collagen and non-collagenous elements, such as glycosaminoglycans, proteoglycans, cytokines, growth factors and their receptors [18,19]. In vertebrates, MMPs consist of > 20 different types of enzymes that differ in tissue expression, cell localization and substrate specificity. MMPs determine ECM equilibrium in normal tissues, or the development of fibrosis under pathological conditions [20]. Gomez et al. [15] demonstrated by immunocytochemistry the participation of MMP-1 and MMP-2 in the formation of active schistosomiasis granulomas, even during prolonged infections. In schistosomiasis granulomas, the production of MMPs is associated with macrophage activation by parasite antigens [21,22]. In addition, elastase expression (MMP-12) is induced in various liver diseases, including cirrhosis and schistosomiasis [18,22,23].

Currently, there is limited evidence that MMPs are involved in the pathophysiology of *S. mansoni* infection [21,22]. By modulating the immune response induced by antigens of parasite eggs, it is possible that MMPs interfere with granulomatous inflammation, mainly by modulating the collagenogenesis and collagenolysis processes. By modifying the evolution and organization of schistosomiasis granulomas, MMPs can change the most serious pathological process related to high morbidity and mortality rates in *S. mansoni*-infected hosts. Thus, MMPs modulatory drugs may exert a relevant impact on schistosomiasis, with a particular effect on tissue inflammation and fibrosis. In this context, doxycycline (Dx) has already been described as an inhibitor of MMPs activity, and its use has previously been proven in the modulation of tissue levels of collagen in parasitic disease [24]. Although Dx is effective in the treatment of *Plasmodium falciparum* infections [24,25] and several filarial species [26], little is known about the role of Dx in schistosomiasis. Thus, this study used *in vitro* and *in vivo* experimental models to study the effect of doxycycline hyclate in adult *S. mansoni* worms and on the development of hepatic granulomatous inflammation in *S. mansoni*-infected mice.

2. Materials and methods

2.1. In vitro assays

2.1.1. Culture of adult S. mansoni worms

Doxycycline toxicity was evaluated in cultures of adult *S. mansoni* worms. Seven mice subcutaneously infected with 25 *S. mansoni* cercariae (LE strain, Rene Rachou Center, Brazil) were sacrificed 80 days after infection by intraperitoneal administration of 3.0% sodium pentobarbital (0.3 mL). Adult worms were recovered by retrograde liver perfusion in infected mice according to Smithers and Terry [27]. The worms were cultured in 6-well plates containing one pair of worms per well (Ethical approval 26/2018). The culture was stabilized in a 5% CO_2 atmosphere in 1 mL RPMI-1640 medium supplemented with heat-inactivated fetal bovine serum, 1% penicillin (10,000 IU/mL) and streptomycin (10.0 mg/mL) (Sigma, St Louis, MO, USA) [28].

2.1.2. In vitro doxycycline toxicity assay

Adult worms in culture were incubated at 37 °C in 5.0% CO_2 with different concentrations of doxycycline hyclate (Dx; 50, 65, 80, 95, 110, 125, 150, 165 and 180 μg/mL). Worms incubated in RPMI-1640 culture medium alone or treated with a cytotoxic reference dose of Pz (2.0 μg/mL) were used as negative and positive controls, respectively [28]. Incubation with the drugs was performed for 24 h. The worms were then washed with culture medium to remove the drugs and kept under the same culture conditions for eight days.

On the first day of incubation, the worms were observed under an inverted microscope (Eclipse ts100, Nikon, Tokyo, Japan) at 2 and 24 h after addition of the drugs. After washing and changing the culture medium, the worms were examined daily for seven days. During this period, parameters such as (i) mating rate, (ii) eggs laying, (iii) egg microstructure, (iv) contraction rate, and (iv) mortality rate of worms were evaluated. The effective lethal dose required to kill 50% of worms (LD_{50}) was calculated using GraphPad Prism software (La Jolla, CA, USA). All experiments were performed using six independent replicates.

2.1.3. Evaluation of doxycycline-induced integumentary damage

Integumentary lesions in adult *S. mansoni* worms were evaluated by scanning electron microscopy. After the toxicity test, the worms were collected and fixed for 24 h in 2.5% glutaraldehyde solution. The worms were dehydrated in a series of increasing concentrations of ethanol (50 to 99.5%) and in an oven at 60 °C for 12 h. Afterwards, they were mounted on metallic supports, covered with gold (Modular Balzers Union FDU 010, SCA 010, Oerlikon Balzers, Balzers, Liechtenstein) and examined using a scanning electron microscope (Leo 1430VP; Carl Zeiss, Jena, Thuringia, Germany) [29,30]. The analysis of worm integrity was based on the observation of morphological evidence of integumentary erosion, peeling, bubbles, eruption, changes in surface tubercle structure (collapse, fusion, presence and distribution of spicules), as well as retraction of the worm's body [31,32].

2.2. In vivo assays: animal model of schistosomiasis

2.2.1. Infection and experimental groups

Forty Swiss mice were randomized into the following four groups with 10 animals per group: (i) Control – uninfected; (ii) Infected control - *S. mansoni* infected; (iii) Positive control (reference treatment) - infected with *S. mansoni* and treated with Pz (200 mg/kg); (iv) Doxycycline group - infected with *S. mansoni* and treated with Dx (50 mg/kg). Infected animals were inoculated subcutaneously with 25 cercariae of *S. mansoni* (LE strain, Rene Rachou Center, Brazil). After 80 days of infection, the animals were treated orally with Pz as a single dose [33] or Dx for 60 days. Considering the absence of a reference for schistosomiasis, Dx was administered daily with a dose that was capable of inducing immunomodulatory effect in a murine model of *Trypanosoma cruzi* infection [34]. Throughout the experiment, the animals were kept in an experiment room with controlled temperature (22 ± 2 °C) and luminosity (12 h/12 h, light/dark cycles). Commercial food and water were provided *ad libitum*. The study was approved by the institution's Ethics Committee for Animal Research (protocol 26/2018).

2.2.2. Euthanasia and necropsy

Twenty-four hours after the final treatment, the animals were euthanized under anesthesia (100 mg/kg ketamine and 10 mg/kg xylazine by i.p. injection) for collection of blood and liver samples. Blood was centrifuged in the presence of anticoagulant (sodium heparin) at 3000 × *g* and 4 °C for 15 min. Blood plasma was collected for analysis liver function enzymes and cytokines. The liver was weighed and the hepatosomatic index was calculated by dividing the liver mass by the

body mass [35]. Samples of liver tissue (300 mg) were frozen (−80 °C) for subsequent determination of MMP-2 and MMP-9 activities. For the histopathological and stereological analysis, liver fragments (median lobe) were fixed in 4% buffered paraformaldehyde solution (pH = 7.4, 0.1 M) for 48 h [35].

2.2.3. Analysis of hepatic function and systemic inflammation

Plasma samples were used for the biochemical analysis of the liver function enzymes aspartate aminotransferase (AST), alanine aminotransferase (ALT), and alkaline phosphatase (ALP) [36]. The analyses were performed by a colorimetric method using a spectrophotometer, according to the instructions provided by the manufacturer of the diagnostic kits used (Human *in Vitro* Diagnostics, Minas Gerais, Brazil). C-reactive protein (CRP) was used as a biochemical marker of systemic inflammation. CRP analysis was performed using spectrophotometry. For this, a 96-well ELISA immunoenzymatic diagnostic kit was used (analytical sensitivity < 10 pg/mL), according to instructions provided by the manufacturer (ThermoFisher Scientific, Waltham, MA, USA).

2.2.4. Quantification of hepatic cytokine levels

Liver samples (median lobe) were homogenized in the presence of protease inhibitor (Protease Inhibitor Cocktail; Sigma-Aldrich, USA) and centrifuged at 3000 ×*g*, 4 °C for 15 min. The supernatant was collected for the quantification of interleukin-4 (IL-4), interleukin-10 (IL-10), tumor necrosis factor-α (TNF-α) and transforming growth factor β (TGF-β). The analysis was conducted by flow cytometry bead array (CBA) using a commercial kit according to the manufacturer's instructions (BD Biosciences, San Diego, CA, USA). Data were collected using a FACSVerse flow cytometer and analyzed using FCAP 3.0 software. Standard curves were generated for each recombinant cytokine in a concentration range 20 to 5000 pg/mL. According to the manufacturer, the lower limit of cytokine detection by CBA was 2.5 to 52.7 pg/mL, depending on the analyte [37].

2.2.5. Tissue processing for bright field and polarization microscopy

After histological fixation (4% formaldehyde (w/v) in 0.1 M phosphate buffer, pH 7.2 for 48 h), liver fragments were dehydrated in increasing concentrations of ethanol (70 to 99.8%). They were then diaphanized in xylene and embedded in paraffin. The blocks were cut into semi-series at 5-μm thickness [38]. Histological sections with a distance of 100 μm were collected to avoid analyzing the same histological area. The sections were stained by the hematoxylin and eosin technique for general histopathological [39] and stereological analysis [35]. Sections stained using the Sirius Red method were used for identification and analysis of collagen fibers under polarization microscopy [40]. Liver sections were stained using the Periodic acid-Schiff histochemical method for glycogen identification and analysis [41]. The sections were mounted with a coverslip and visualized using a photomicroscope (Axioscope A1, Carl Zeiss, Germany). Ten histological images were obtained for each animal and each staining method using Axion Vision LE image capture and analysis software (Carl Zeiss, Germany).

2.2.6. Liver histopathological analysis

Histopathological evaluation was carried out in a qualitative way, observing evidence of tissue necrosis, cellular hypertrophy/hypotrophy, cytoplasmic glycogen inclusion pattern, organization and distribution of parenchymal and stromal cells, morphology and distribution of blood vessels and interstitial cells, as well as the presence and distribution of inflammatory foci, Schistosomiasis granulomas and areas of tissue fibrosis [40]. The analysis was performed in 10 random histological fields for each animal using a ×40 objective lens (×400 magnification), with examination of 21.10×10^5 μm^2 total histological area for each group [40].

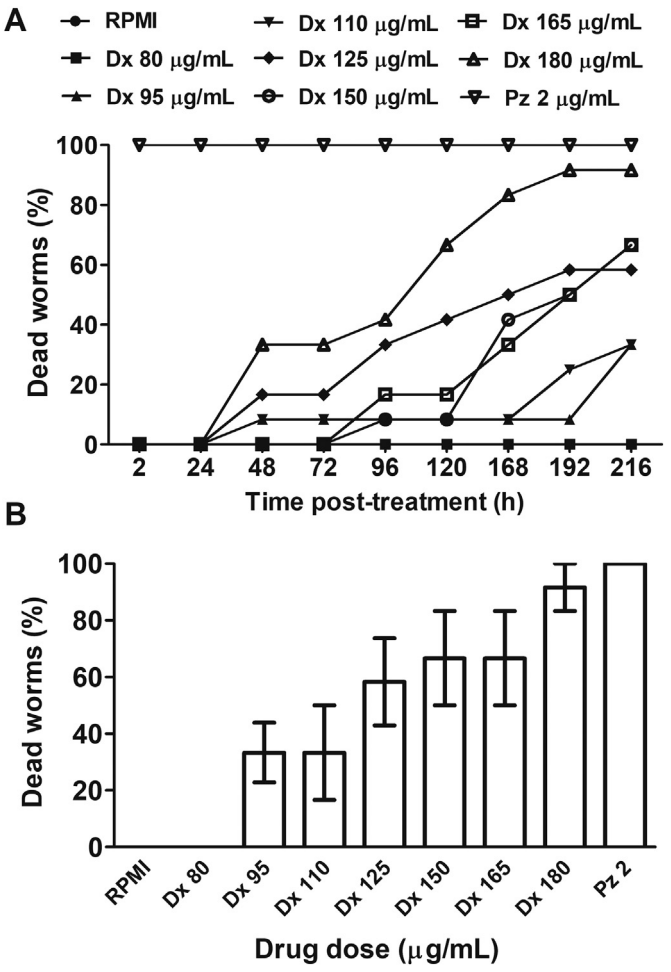

Fig. 1. Cumulative mortality of adult *Schistosoma mansoni* worms untreated and treated with different doses of doxycycline hyclate. (A) Daily mortality after doxycycline treatment. (B) Accumulated mortality 216 h after contact of parasites with different doxycycline doses. RPMI: RPMI-1640 culture medium, Dx: doxycycline hyclate (80, 95, 110, 125, 150, 165, and 180 μg/mL), Pz (positive control): praziquantel (2 μg/mL).

2.2.7. Stereological and histomorphometric analysis of hepatic granulomas

The number density of granulomas per unit of histological area (QAG, n/mm^2) was evaluated using the stereological formula $QA_G = \Sigma G/At$; where Σ*G* represents the sum of the number of granuloma profiles and *At* corresponds to the size of the test area (34×103 μm^2). The QA_G was evaluated from 10 random non-coincident histological fields for each animal obtained with a ×5 objective lens (×50 magnification), in a 27.20×10^7 μm^2 total histological area for each group. Exudative-productive and organized granulomas (fibrotic) were quantified differentially according to a previously established morphological characterization [42].

The area of the equatorial section of the granulomas was directly determined by a histomorphometric method using the contour tool of the Image-Pro plus 4.5 image analysis program (Media Cybernetics Inc., Silver Spring, Maryland, USA) [38]. Mean granuloma volume was estimated by the principle of prolate (P) spheroid, according to the formula VP = (4/3) ∗ πa2b; where *a* is the equatorial (smaller) radius and *b* is the polar (larger) radius of the cross-sectional profile of a spheroidal structure (JO et al., 2007). One hundred granulomas were analyzed per group, within which an *S. mansoni* egg was clearly observed [42].

2.2.8. Stereological analysis of inter-granulomatous liver tissue

In areas of liver tissue that were remote from the granulomas, the amplitude of hepatic microstructural remodeling was estimated by

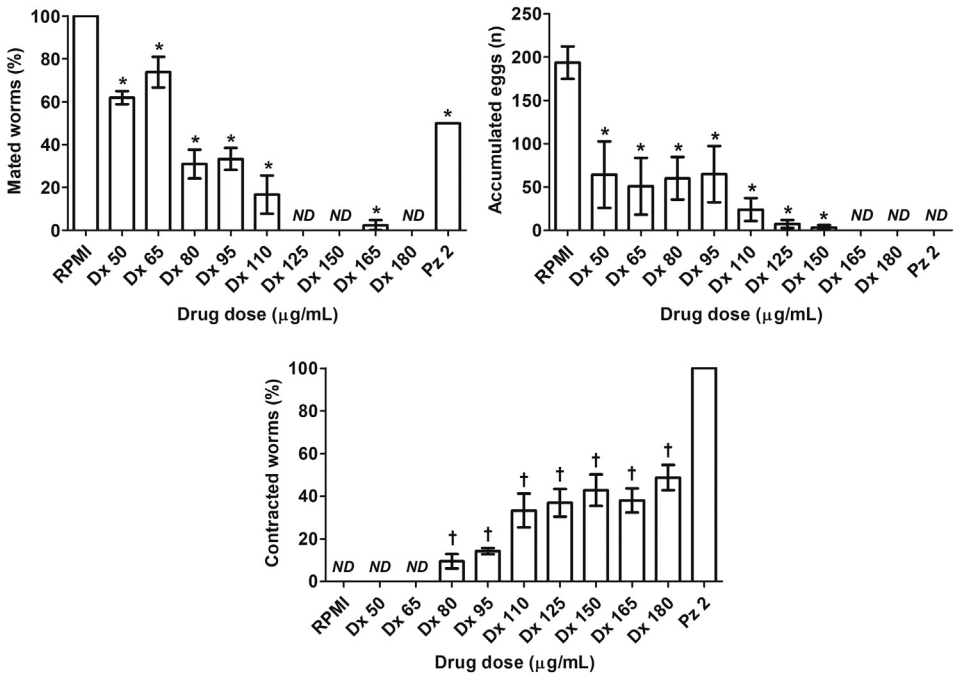

Fig. 2. Rate of mated worms, accumulated eggs, and contracted worms in adult *Schistosoma mansoni* worms treated and untreated with different doses of doxycycline hyclate. Data representative of the end of 216 h (observation period) after parasites contact with different doxycycline doses. RPMI: RPMI-1640 culture medium, Dx: doxycycline hyclate (50, 65, 80, 95, 110, 125, 150, 165, and 180 μg/mL), Pz (positive control): praziquantel (2 μg/mL). ND: not detected. The results are represented as median and interquartile range. Statistical difference ($P < 0.05$) in relation to the group, † RPMI, Dx 50 and Dx 65.

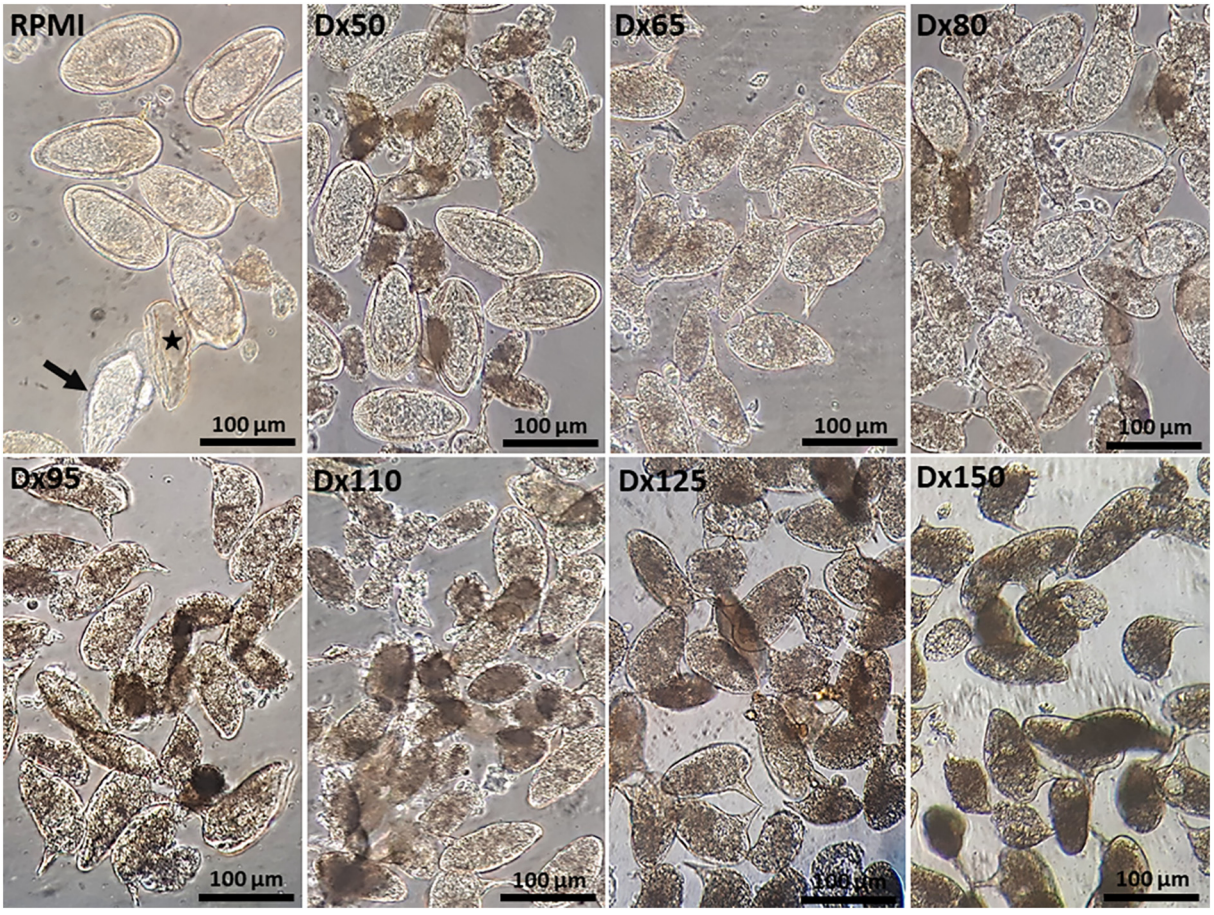

Fig. 3. Phase contrast photomicrographs of *Schistosoma mansoni* eggs accumulated at the end of 216 h (observation period) after administration of doxycycline hyclate. RPMI: RPMI-1640 culture medium, Dx: doxycycline hyclate (50, 65, 80, 95, 110, 125, 150 μg/mL). No eggs were identified when parasites were cultured with Pz or 165 and 180 μg/mL Dx. The images indicate dose-dependent degeneration of *S. mansoni* eggs. Arrow: Newly hatched miracidium separating from the eggshell (star).

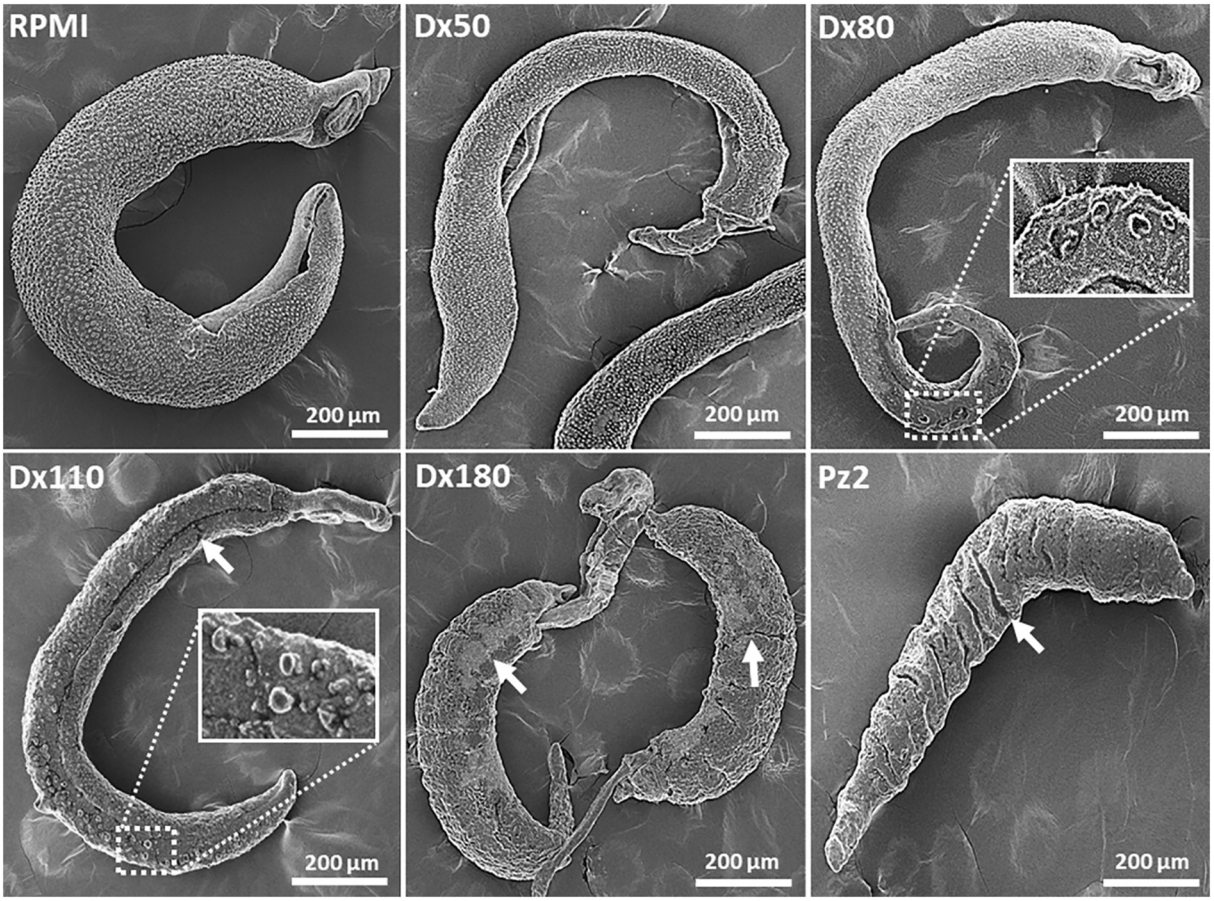

Fig. 4. Scanning electron photomicrographs of adult *Schistosoma mansoni* worms untreated and treated with doxycycline hyclate. Images obtained 216 h (period of observation) after the contact of parasites with different doxycycline doses. Control group (RPMI): RPMI-1640 culture medium, Dx: doxycycline hyclate (80, 95, 110, 125, 150, 165, and 180 µg/mL), Pz (positive control): praziquantel (2 µg/mL). Featured images: Dx 80, tegument erosion; Dx 110, bubbles and tegument erosion. Arrows: areas of integument contraction.

using the stereological method [40,43]. The volume density (hepatocytes [parenchyma], connective tissue [stroma], sinusoidal capillaries and cytoplasmic glycogen inclusions) and number density (hepatocytes and interstitial/inflammatory cells) were estimated according to stereological principles previously described [40]. The volume density (Vv, %) was estimated by counting points according to the formula $Vv = \Sigma P/Pt$; where ΣP represents the number of test points hitting the structure of interest and Pt is the total number of points in the test system. A quadratic test system with 100 points contained in a $42.21 \times 10^3\,\mu m^2$ test area (At) at tissue level was used. The number density (QA, n/mm^2) was evaluated by the same principle described above for the quantification of the number of granulomas per unit of liver area. The stereological analysis was performed in 10 random, non-coincident, histological fields for each animal, obtained with a ×40 objective lens (×400 magnification) in a $21.10 \times 10^5\,\mu m^2$ total microscopic area for each group. All analyses were performed using Image-Pro Plus 4.5 image analysis software (Media Cybernetics Inc., Silver Spring, Maryland, USA) [43].

2.2.9. Evaluation of MMP-2 and MMP-9 hepatic activity

For the evaluation of MMP-2 and MMP-9 activity, 200-mg samples of the liver were homogenized in 1 mL of 5 mM Tris-HCl (pH 7.4) buffer containing 0.15 M NaCl, 10 mM $CaCl_2$ and 0.02% NaN_3. After centrifugation at 10,000 ×*g* for 30 min, the supernatant was collected for analysis of MMP activity. For this, an ELISA commercial immunoenzymatic kit was used according to the manufacturer's instructions (ABCAM, Cambridge, MA, USA). The overall activity of each MMP was determined by the difference between the general enzymatic activity and the enzymatic activity obtained after homogenate treatment with specific inhibitors of MMP-2 (cis-9-Octadecenoyl-*N*-hydroxylamide) (Sigma-Aldrich, St. Louis, Missouri, USA) and MMP-9 (2-(*N*-benzyl-4-methoxyphenylsulfonamido)-5-((diethylamino) methyl)-*N*-hydroxy-3-methylbenzamide) (ABCAM, Cambridge, MA, USA).

2.3. Statistical analysis

The results were expressed as absolute values, percentages, mean and standard deviation (mean ± SD), or median and interquartile range. Normality in the data distribution was assessed using the Kolmogorov-Smirnov test. The data variance was measured by one-way ANOVA. Parametric data were submitted to the Student-Newman-Keuls post-hoc test for multiple comparisons. Non-parametric data were compared using the Kruskal-Wallis test. The results with P value < 0.05 were considered statistically significant.

3. Results

3.1. Doxycycline hyclate induces dose-dependent toxicity in vitro in adult S. mansoni worms

In vitro assays indicated dose- and time-dependent Dx toxicity in *S. mansoni* adult worms. No deaths were observed at 80 µg/mL and 91.7% mortality was recorded at a dose of 180 µg/mL. The LD_{50} was determined as 112.0 µg/mL Dx. All worms (100%) died after treatment with Pz (Fig. 1).

Adult worms in culture medium had a high rate of mating and eggs

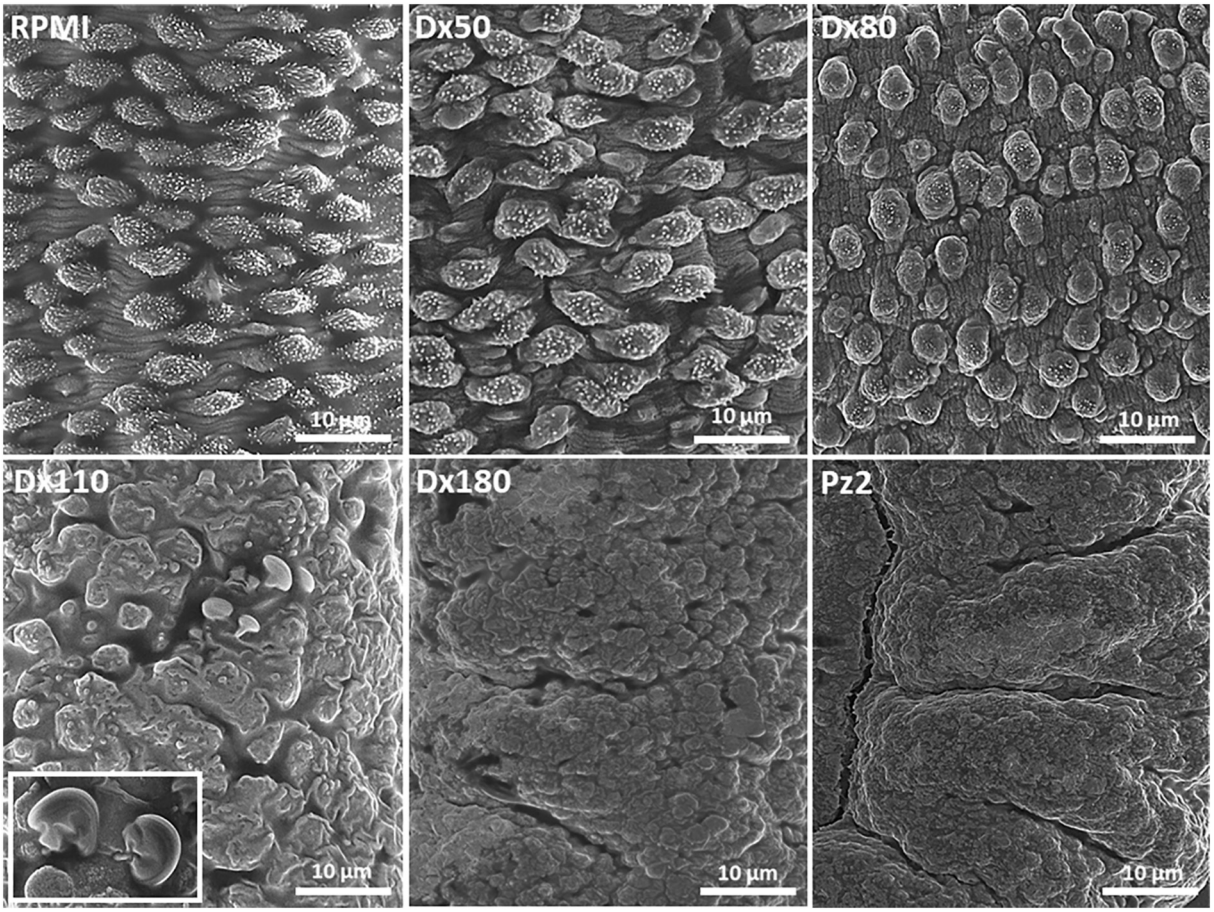

Fig. 5. Scanning electron photomicrographs of the integument of adult *Schistosoma mansoni* worms untreated and treated with doxycycline hyclate. Images obtained 216 h (period of observation) after the contact of parasites with different doxycycline doses. (Control): RPMI-1640, Dx: doxycycline hyclate (80, 95, 110, 125, 150, 165 and 180 µg/mL), Pz (positive control): praziquantel (2 µg/mL). RPMI and Dx50: integument with preserved morphology, showing prominent tubers and well-defined spicules; Dx80: tuber flattening and spike density reduction; Dx110: collapse of tubers, disappearance of spicules, and bubbles in the integument (highlighted image); Dx180 and Pz2: tubercle collapse, spicule disappearance and integumentary contraction bands.

laying, and an absence of integumentary contraction. Mating rate and eggs laying presented a significant dose-dependent reduction in Dx-treated groups compared to control worms ($P < 0.05$). About 50% of the dead worms remained mated in the group treated with Pz. In contrast, the rate of worm contraction presented a significant and dose-dependent increase compared to the control worms ($P < 0.05$; Fig. 2).

Phase-contrast microscopy indicated that, under control conditions (worms grown in RPMI-1640 medium), *S. mansoni* eggs had a normal structure with well-defined spicules and intense miracidium motility within the egg. Empty eggshells and free miracidium were also observed. Dx-induced eggs degeneration (smaller size, loss of the border between the embryo and the eggshell, and embryo with lumpy appearance, vacuolated and without ciliary movement) showed dose-dependent characteristics. No eggs were identified when the parasites were cultured with Pz or with Dx at 165 and 180 µg/mL (Fig. 3).

Control worms kept in culture medium presented complete morphological integrity. In Dx-treated worms, dose-dependent microstructural damage of the cephalic pole and integument were detected. Microstructural changes of the integument, such as blistering, erosion, desquamation and contraction bands, as well as retraction of the worms' bodies and atrophy of the cephalic pole were more evident at Dx concentrations higher than 80 µg/mL. At 180 µg/mL Dx and in worms treated with Pz, these changes were more pronounced (Fig. 4).

Detailed morphological analysis of the *S. mansoni* integument revealed a preserved structure in control worms and in worms treated with the lowest Dx dose (50 µg/mL). At higher Dx doses, the microstructural integumentary alterations presented dose-dependent characteristics. The most important integumentary alterations were the disappearance of the spicules; flattening, collapse and disappearance of tubers; disappearance of inter-tubercular striae; erosion; blisters; contraction bands and integumentary folds (Fig. 5).

3.2. Doxycycline hyclate modulates granulomatous inflammation and hepatic microstructural remodeling in S. mansoni-infected mice

At the end of the experiment, body mass of untreated and Dx-treated infected animals was lower in relation to the control group and infected animals treated with Pz ($P < 0.05$). All infected groups had a higher absolute and relative liver mass compared to uninfected control animals ($P < 0.05$). These parameters were higher in untreated and Dx-treated infected animals compared to the Pz-treated group ($P < 0.05$; Fig. 6).

Uninfected animals presented normal hepatic microstructure, with well-defined hepatocyte strings, well-delimited sinusoidal capillaries, low interstitial cellularity, and absence of morphological evidence of cellular degeneration. In the area that was remote from the granulomas, all infected animals presented marked hepatic inflammation, with diffuse leukocyte infiltrate and areas with well-defined inflammatory foci. These animals also showed expansion of the connective stroma and marked dilation of sinusoidal capillaries (Fig. 7).

All infected animals showed a significant increase in circulating AST, ALT, ALP and CRP levels compared to control animals ($P < 0.05$). In general, these parameters were similar in untreated and Dx-treated infected animals ($P > 0.05$), but higher in relation to Pz-treated mice ($P < 0.05$; Table 1).

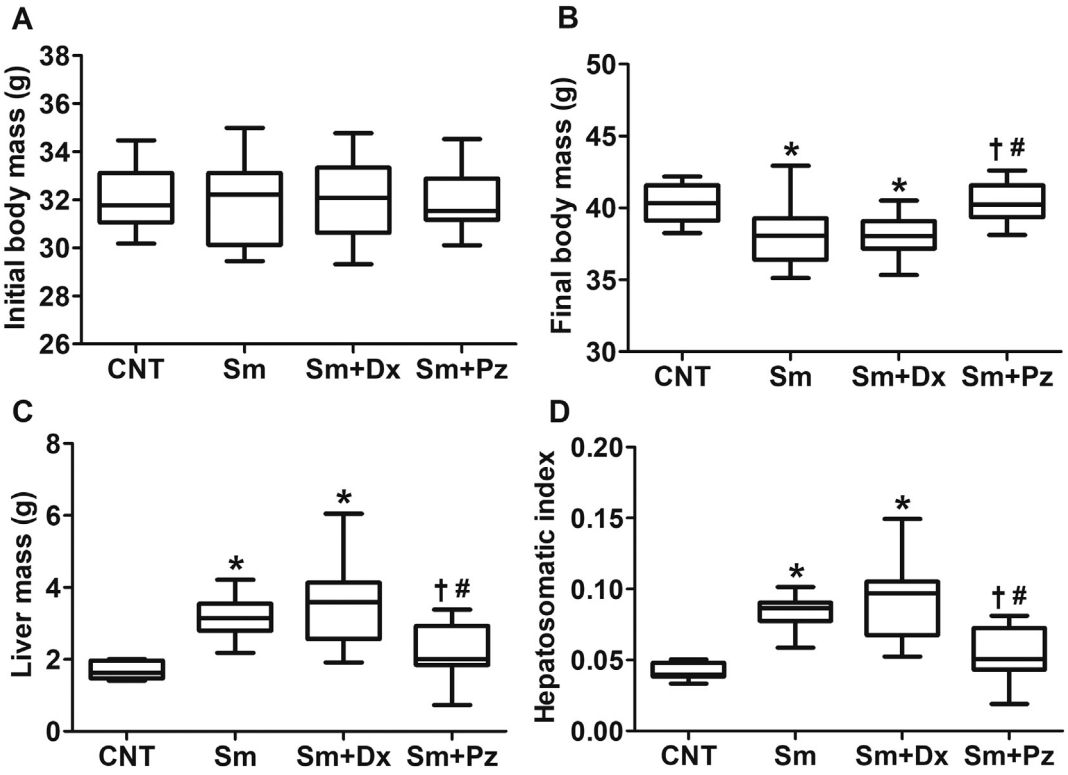

Fig. 6. Body mass, absolute and relative liver mass (hepatosomatic index) in *Schistosoma mansoni*-infected mice untreated and treated with doxycycline (Dx) and praziquantel (Pz). CNT: uninfected control, Sm: infected with *S. mansoni*, Sm + Pz: infected with *S. mansoni* and treated with a single dose of Pz (200 mg/kg), Sm + Dx: infected with *S. mansoni* and treated for 60 days with Dx (50 mg/kg/day). The results are represented as median and interquartile range. Statistical difference ($P < 0.05$) in relation to the group *CNT, †Sm, #Sm + Dx.

All infected animals showed a significant increase in IL-4, IL-10, TNF-α and TGF-β levels compared with uninfected animals ($P < 0.05$). Dx-treated animals showed elevated IL-4 levels compared to untreated infected animals ($P < 0.05$). Pz-treated animals had lower levels of all cytokines than untreated and Dx-treated infected animals ($P < 0.05$; Fig. 8).

Hepatocytes from uninfected animals showed marked glycogen accumulation. Evident cytoplasmic depletion of hepatic glycogen inclusions was observed in all infected animals, especially in untreated and Dx-treated infected animals (Fig. 9).

Quantitative microstructural analysis of the intergranulomatous liver tissue corroborated the qualitative evidence of hepatic connective stromal expansion, sinusoidal capillary dilation, increased inflammatory cell density and hepatic glycogen depletion in all infected groups compared to uninfected animals ($P < 0.05$; Fig. 10). Capillary volume density was similar in all infected groups ($P > 0.05$; Fig. 10). Connective tissue expansion and leukocyte infiltration were more pronounced in infected animals treated with Dx compared to the other infected groups ($P < 0.05$). Pz-treated animals presented higher hepatic glycogen distribution compared to untreated and Dx-treated infected animals ($P < 0.05$; Fig. 10).

Quantitative microstructural analysis indicated that granuloma number, mean diameter, cross-sectional area and volume were similar in both untreated and Dx-treated infected animals ($P > 0.05$). All these parameters were significantly lower in Pz-treated animals ($P < 0.05$; Fig. 11).

All *S. mansoni*-infected animals presented marked granulomatous inflammation. Untreated and Dx-treated infected animals showed intense leukocyte infiltration and large granulomas with high cellularity, with typical morphological characteristics of exudative-productive granulomas. In Pz-treated animals, granulomas presented a less pronounced cellularity and marked accumulation of eosinophilic amorphous material around *S. mansoni* eggs, indicating an involutive morphological profile (Fig. 12).

Hepatic granulomas presented variable collagen accumulation. In general, untreated infected animals presented collagen fibers at different stages of development (type I and III), with little compaction and diffuse distribution. Pz-treated animals presented higher accumulation of thick collagen fibers (type I) with a higher degree of compaction and circumferential organization around *S. mansoni* eggs. In Dx-treated animals, marked deposition of thicker collagen fibers with diffuse organization was observed (Fig. 12).

Untreated infected animals had a higher proportion of exudative-productive granulomas compared with Dx- or Pz-treated groups. The proportion of exudative-productive (53.25%) and involutive granulomas (46.75%) in the Dx-treated animals was similar, whereas Pz-treated animals had a higher proportion of involutive granulomas compared to the other groups ($P < 0.05$; Fig. 13). The relative distribution of collagen per granuloma area was similar in Dx- or Pz-treated animals ($P > 0.05$), which demonstrated higher collagen deposition compared to untreated infected animals ($P < 0.05$; Fig. 13).

Immunoenzymatic analysis indicated that untreated and Pz-treated infected animals had a significant increase in liver MMP-2 and MMP-9 activity compared to control mice ($P < 0.05$). MMP-2 activity was reduced ($P < 0.05$) and MMP-9 activity was similar ($P > 0.05$) in Dx-treated infected animals compared to uninfected animals (Fig. 14).

4. Discussion

The present study used an integrated *in vitro* and *in vivo* strategy to evaluate the schistosomicidal potential of Dx and the impact of this drug on the evolution of granulomatous inflammation induced by *S. mansoni* in mice. Our *in vitro* findings indicated that Dx is potentially toxic to adult *S. mansoni* worms. In addition to interfering with mating, eggs laying and viability of these eggs, Dx was able to induce dose-dependent integumentary morphological lesions, with similarities to Pz

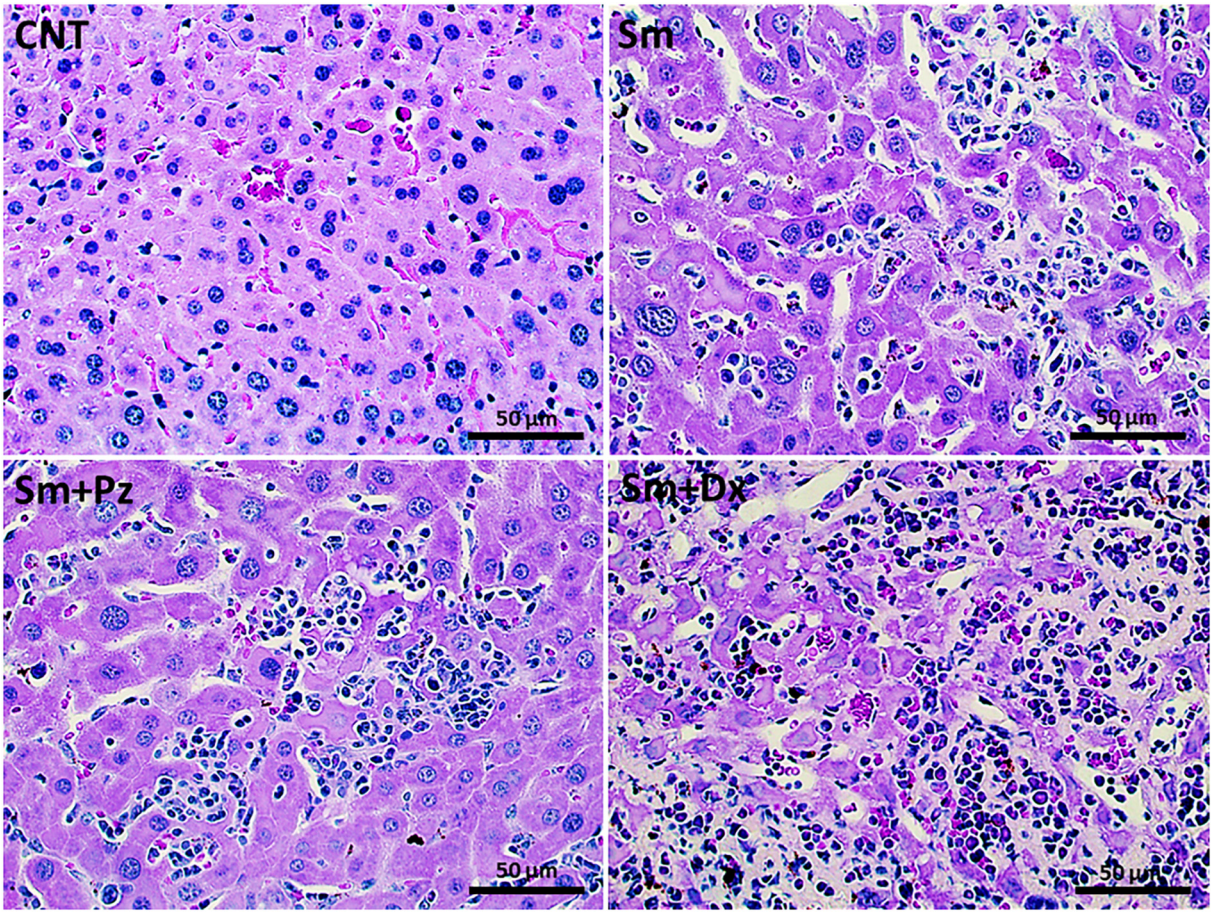

Fig. 7. Representative photomicrographs of remote liver areas (intergranulomatous tissue) in uninfected mice, and *Schistosoma mansoni*-infected animals untreated and treated with doxycycline (Dx) and praziquantel (Pz). CNT: uninfected control, Sm: infected with *S. mansoni*, Sm + Pz: infected with *S. mansoni* and treated with a single dose of Pz (200 mg/kg), Sm + Dx: infected with *S. mansoni* and treated for 60 days with Dx (50 mg/kg/day). Staining method: hematoxylin and eosin, bright-field microscopy.

Table 1
Plasma biochemical markers of hepatic function and systemic inflammation in uninfected mice, and *Schistosoma mansoni*-infected animals untreated and treated with doxycycline (Dx) and praziquantel (Pz).

Groups	AST (IU/L)	ALT (IU/L)	ALP (IU/L)	CRP (mg/L)
CNT	116.82 ± 8.52	25.01 ± 7.69	47.41 ± 8.11	0.19 ± 0.05
Sm	203.99 ± 31.32*	68.43 ± 11.16*	70.01 ± 7.99*	0.67 ± 0.17*
Sm + Dx	213.24 ± 26.96*	75.92 ± 17.91*	74.87 ± 11.82*	0.75 ± 0.12*
Sm + Pz	147.89 ± 16.57*,†	42.48 ± 8.78*,†	47.68 ± 13.18	0.47 ± 0.07*,†

ALT: alanine aminotransferase; AST: aspartate aminotransferase; ALP: alkaline phosphatase; CRP: C-reactive protein. CNT: uninfected control, Sm: infected with *S. mansoni*, Sm + Pz: infected with *S. mansoni* and treated with a single dose of Pz (200 mg/kg), Sm + Dx: infected with *S. mansoni* and treated for 60 days with Dx (50 mg/kg/day). The results are represented as mean and standard deviation. Statistical difference ($P < 0.05$) in relation to the group *CG, †Sm and Sm + Dx.

treatment that partially explain the high parasite mortality rates obtained in response to higher Dx doses (> 110 µg/mL).

Due to its potent bacteriostatic properties, Dx has been effectively used as a broad-spectrum antibiotic for the treatment of diseases such as pneumonia, cholera, syphilis, leptospirosis and chlamydia infections [44,45]. Although the impact of Dx on worms of the genus Schistosoma is still poorly explored, this drug has a direct toxic effect against several parasites with medical relevance. Dx is used in the treatment of malaria in combination with quinine, exhibiting effective action against *Plasmodium falciparum* [24]. In addition, it has been prominent among the new antifilariae drugs, whose effects against bacteria of the genus Wolbachia are considered to be an advance in filariasis treatment [83]. The antimicrobial effects of Dx are mainly mediated by the inhibition of protein synthesis [46], as well as blocking embryogenesis in adult *Onchocerca volvulus* nematode worms [26] and direct macrofilaricidal properties in patients with lymphatic filariasis ([47], [84]). Corroborating the evidence of Dx toxicity in different pathogens, our *in vitro* findings also indicated schistosomicidal activity, being able to kill 50% of adult *S. mansoni* worms at 112 µg/mL. In addition to the effect of Dx on *S. mansoni* mortality, the reproductive capacity of these worms was also impaired, even at doses lower than the LD_{50}, with a significant reduction in the mating rate, posture and/or viability of eggs from 50 µg/mL. Although Dx is a widely used, low cost and readily available antibiotic, its schistosomicidal potential has been neglected for decades. Thus, our findings of toxicity may represent the first evidence of *S. mansoni* pharmacological sensitivity to Dx.

An interesting schistosomicidal potential has been attributed to different antibacterial drugs. There is evidence that antimicrobial compounds based on thiazole and phthalimide showed *in vitro* inhibitory effects on eggs laying in adult *S. mansoni* worms [48].

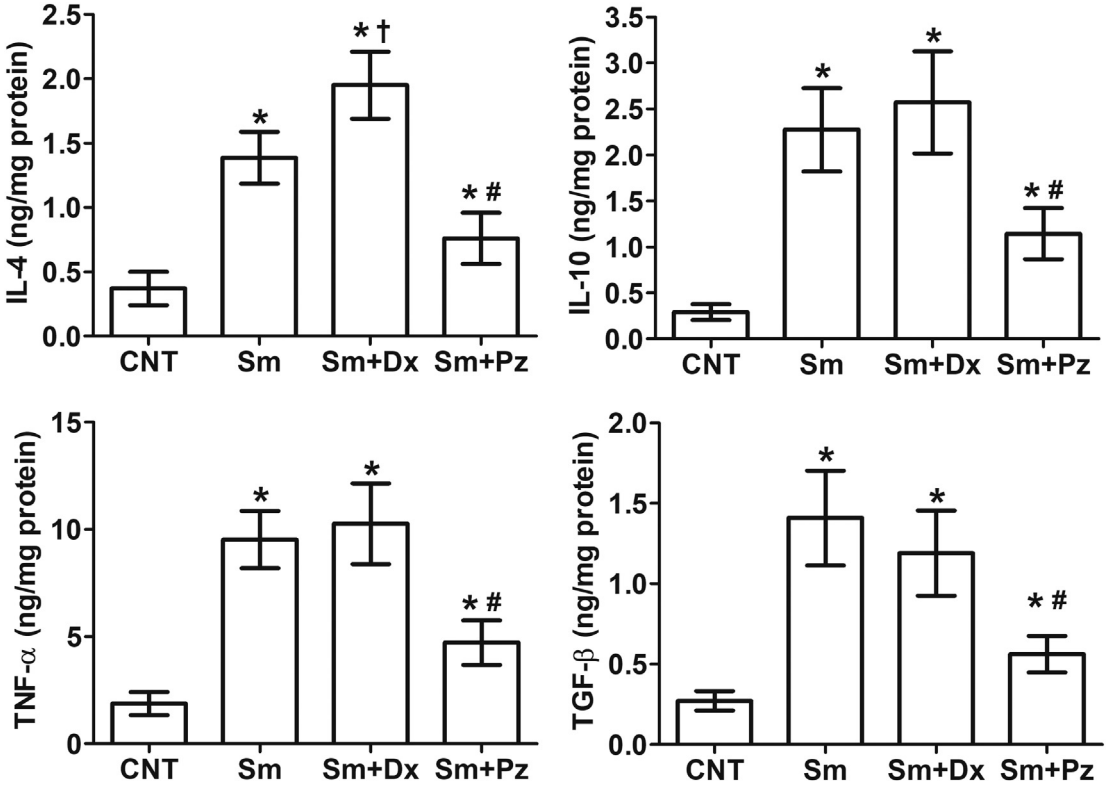

Fig. 8. Hepatic cytokine levels in uninfected mice, and *Schistosoma mansoni*-infected animals untreated and treated with doxycycline (Dx) and praziquantel (Pz). CNT: uninfected control, Sm: infected with *S. mansoni*, Sm + Pz: infected with *S. mansoni* and treated with a single dose of Pz (200 mg/kg), Sm + Dx: infected with *S. mansoni* and treated for 60 days with Dx (50 mg/kg/day). The results are represented as mean and standard deviation. Statistical difference ($P < 0.05$) in relation to the group *CG, †Sm, #Sm and Sm + Dx.

Secondary antibacterial metabolites derived from plants, such as *Allium sativum* [85], [49] and *Zingiber officinale* [49,50], also presented toxic effects in *S. mansoni*, with a negative impact on oviposition rates. Although Dx is toxic to adult *S. mansoni* worms, the mechanisms of toxicity caused by this drug are poorly understood. However, more severe and heterogeneous integumentary alterations were detected in the groups exposed to Dx doses that induced higher parasite mortality rates (> 80.0 μg/mL). Thus, electron microscopy indicated a broad spectrum of dose-dependent morphological lesions in *S. mansoni*, which were predominantly characterized by the flattening or disappearance of spicules and tubers, and by the presence of bubbles, desquamation, erosion and contraction bands in the integument. As Dx-induced microstructural changes were similar to those observed in parasites treated with the reference schistosomicidal drug (Pz), integumentary damage cannot be ruled out as a potential mechanism associated with Dx toxicity in *S. mansoni* worms. Similar integumentary effects were also described in a previous study with Pz [51].

As integument integrity is essential for *S. mansoni* survival, the integument has been an important target for the development of schistosomicidal drugs [52,53]. Most of the drugs currently used against Schistosoma parasites, including Pz [54], [86], mefloquine [55] and artemether [56], exhibit efficacy directly linked to the induction of integumentary lesions in *S. mansoni*. Due to its morphological and molecular complexity, the integument plays an important role during the infection of the definitive host. The integument protects the parasite against immune defense mechanisms of the host, which include the action of antibodies, complement proteins, proteases, as well as reactive oxygen (ROS) and nitrogen (RNS) species produced from the recruitment and activation of leukocytes in the parasitized organs [53]. Although integumentary alterations are linked to the efficacy of schistosomicidal drugs ([54,56], [86], [55]), *S. mansoni* mortality was also detected with Dx doses unable to induce extensive integumentary lesions (< 80.0 μg/mL). Thus, it is possible that the mechanisms of Dx toxicity are more complex than an action limited to the parasite integument, an issue that requires further study.

Despite *in vitro* schistosomicidal efficacy, our *in vivo* findings did not indicate a similar benefit of Dx on hepatic granulomatous inflammation. Consistent with the typical clinical manifestations of schistosomiasis [2,4,57], untreated infected animals presented intense loss of body mass, hepatomegaly, impaired liver function (transaminases) and intense inflammatory processes (CRP and cytokines); these parameters were attenuated by treatment with Pz but not with Dx. As expected, Pz was effective in reducing inflammation and hepatic morphofunctional remodeling, which were more severe and diffuse in the Dx-treated group. In this group, intense leukocyte infiltration and cytokine production was accompanied by marked parenchymal degeneration, expansion of the connective stroma and damage to the hepatocyte membrane, which was evidenced by the elevated circulating levels of AST and ALT.

Hepatic pathological remodeling is directly associated with regional recruitment of leukocytes and the activation of an immune response by antigens from *S. mansoni* eggs retained in the liver [2,13,58]. In fact, intense interstitial cellularity was accompanied by elevated hepatic levels of IL-4, IL-10, TNF-α and TGF-β in infected animals. In general, intense pathological reaction of the liver parenchyma and stroma in schistosomiasis is triggered by the secretion of Th2 inflammatory mediators (*i.e.*, IL-4, IL-5 and IL-6) and T regulatory cells (IL-10 and TGF-β), as well as intense ROS and protease production by activated leukocytes [59,60]. In addition to the recognized toxic effect of ROS and RNS in hepatocytes [61,62], molecules such as IL-4, IL-6 and TGF-β have been implicated in the development of hepatitis and activation of cell death pathways in these cells [63,64]. Interestingly, IL-4 reached higher levels in the Dx-treated animals. This molecule is the main interleukin produced in schistosomiasis responsible for Th2

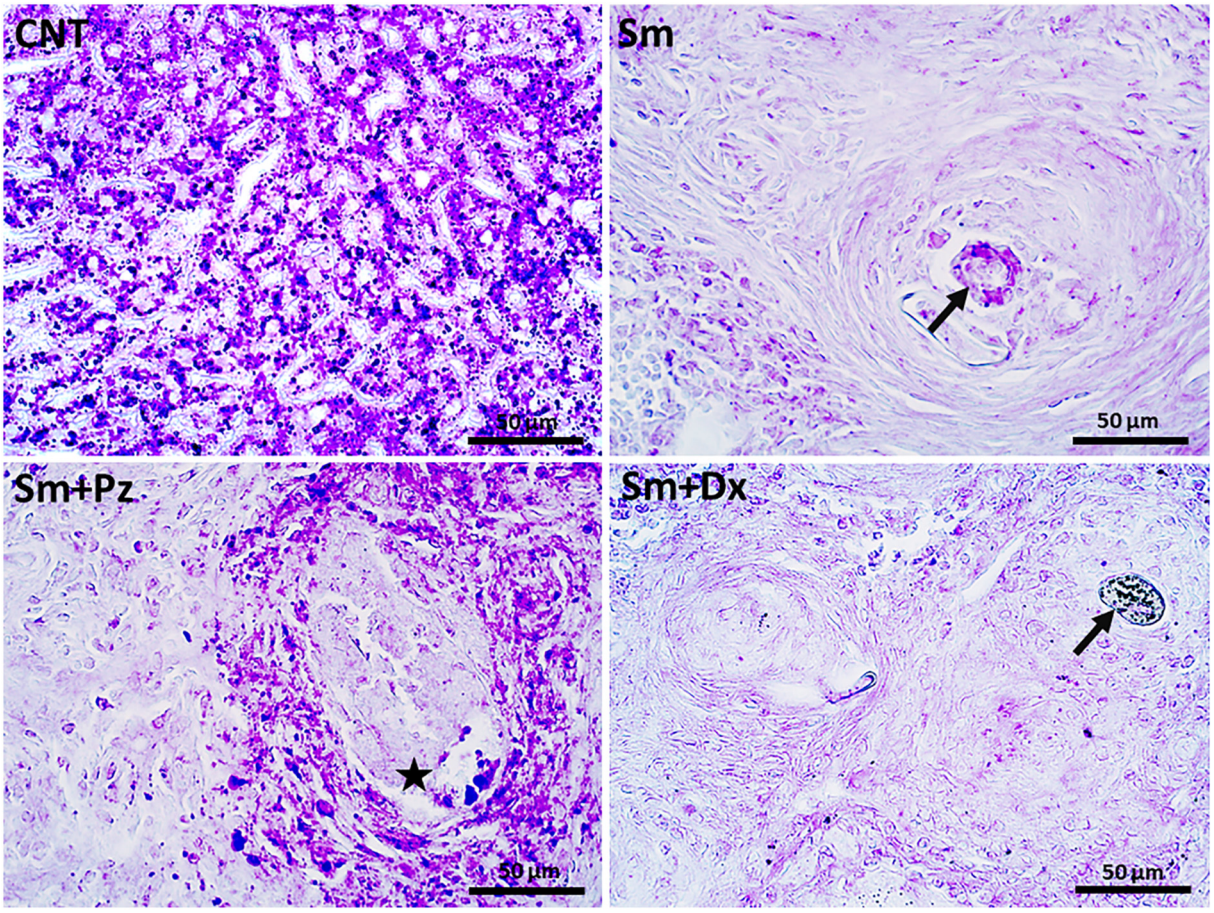

Fig. 9. Representative photomicrographs of the distribution of cytoplasmic glycogen inclusions in hepatocytes in uninfected mice, and *Schistosoma mansoni*-infected animals untreated and treated with doxycycline (Dx) and praziquantel (Pz). CNT: uninfected control, Sm: infected with *S. mansoni*, Sm + Pz: infected with *S. mansoni* and treated with a single dose of Pz (200 mg/kg), Sm + Dx: infected with *S. mansoni* and treated for 60 days with Dx (50 mg/kg/day). Color: Schiff periodic acid, light field microscopy. Star: hepatic granuloma. Arrow: *S. mansoni* eggs in the center of hepatic granulomas.

immunological polarization [65]. The role of IL-4 in *S. mansoni*-induced parenchymal damage is still poorly understood; however, activation of the IL-4 receptor in hepatocytes has been associated with degeneration and cell death mediated by the caspase pathways in several liver diseases, especially in cases of cirrhosis, autoimmune injury, chronic and viral hepatitis [66–68]. In addition to the potential role of IL-4 in hepatocyte degeneration, this interleukin is involved in the recruitment of monocytes, eosinophils and mast cells [63,65], with a direct impact on the organization of schistosomiasis granulomas [58,65]. Although granulomas are essential for isolating *S. mansoni* eggs and attenuating chronic antigenic stimulation, this protective response occurs at the expense of extensive pathological hepatic remodeling [13,58], which can progress to hepatic failure and host death [2,13].

In addition to hepatic morphological damage, all infected animals, especially those untreated and treated with Dx, showed intense depletion of cellular glycogen stores. This finding indicates that, in addition to subverting the hepatic microstructure, granulomatous inflammation also induced marked metabolic stress in hepatocytes. As treatment with Pz attenuated inflammation and glycogen depletion, both events appear to be related. Although tissue energy metabolism is poorly understood in schistosomiasis, increased production of inflammatory mediators, such as IL-6, TNF-α and prostaglandins, in hepatic inflammatory processes is associated with the activation of glycogenolysis and glycogen depletion in hepatocytes [69,70]. In this sense, in addition to attenuating the production of these mediators and inflammation intensity, steroidal agents such as dexamethasone are effective in restoring hepatic glycogen reserves, corroborating the relationship between inflammation and hepatic energy metabolism [70]. This relationship becomes evident considering that molecules such as glycogen synthase kinase 3 (GSK3) share a central role in glycogen synthesis and regulation of the immune response in eukaryotic cells, modulating the synthesis of anti- (*i.e.*, IL-10) and pro-inflammatory cytokines (*i.e.*, IL-6, IL-12, IFN-γ, and TNF-α) from cell signaling pathways mediated by serine-threonine kinase Akt and nuclear factor kappa B [71,72].

Although untreated and Dx-treated infected animals showed marked differences in the amplitude of pathological liver remodeling, the number and size of granulomas was similar in these groups. On the other hand, reduced granuloma number and size was obtained by treatment with Pz. As expected, these findings indicated reduced oviposition and hepatic retention of *S. mansoni* eggs in Pz-treated animals, an aspect related to the efficacy of this drug in eliminating these parasites [2,73]. In this sense, the predominance of small granulomas in the involutive stage was already expected in Pz-treated animals, indicating a longer period of organization of granulomas around eggs deposited in the liver in the period prior to treatment [13]. On the other hand, the ineffectiveness of Dx in eliminating adult *S. mansoni* worms may partially explain the greater amount of exudative-productive granulomas. In this case, continuous oviposition and eggs retention in the liver can trigger immunological hyperstimulation and intense cellular recruitment, events necessary for the organization of new granulomas, which initially assume a great size due to their exudative-productive aspect [13,42].

Interestingly, Dx- and Pz-treated animals exhibited a similarly high collagen content in the granulomatous sheath compared to untreated

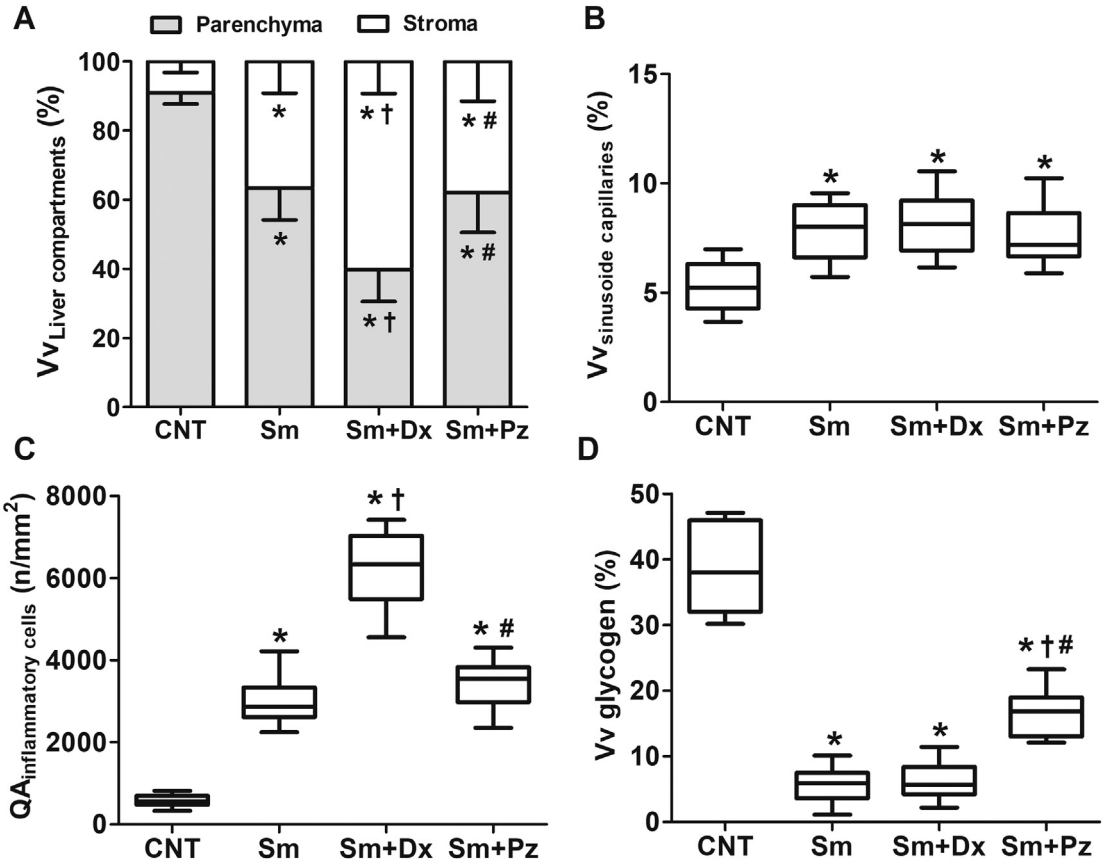

Fig. 10. Volume density (Vv) of parenchyma, stroma, sinusoidal capillaries, and glycogen deposits; and number density (QA) of inflammatory cells in the liver of uninfected mice, and *Schistosoma mansoni*-infected animals untreated and treated with doxycycline (Dx) and praziquantel (Pz). CNT: uninfected control, Sm: infected with *S. mansoni*, Sm + Pz: infected with *S. mansoni* and treated with a single dose of Pz (200 mg/kg), Sm + Dx: infected with *S. mansoni* and treated for 60 days with Dx (50 mg/kg/day). The results are represented as median and interquartile range. Statistical difference ($P < 0.05$) in relation to the group *CG, †Sm, #Sm + Dx.

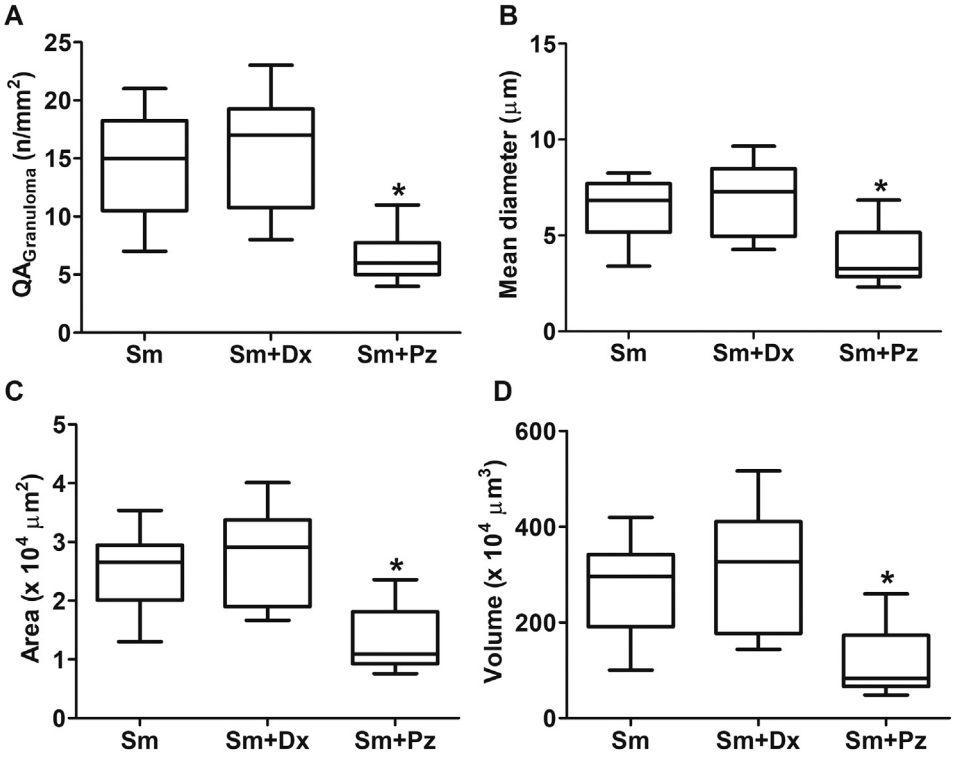

Fig. 11. Number, diameter, area and volume of hepatic granulomas in *Schistosoma mansoni*-infected mice untreated and treated with doxycycline (Dx) and praziquantel (Pz). Sm: infected with *S. mansoni*, Sm + Pz: infected with *S. mansoni* and treated with a single dose of Pz (200 mg/kg), Sm + Dx: infected with *S. mansoni* and treated for 60 days with Dx (50 mg/kg/day). The results are represented as median and interquartile range. *Statistical difference ($P < 0.05$) in relation to Sm and Sm + Dx groups.

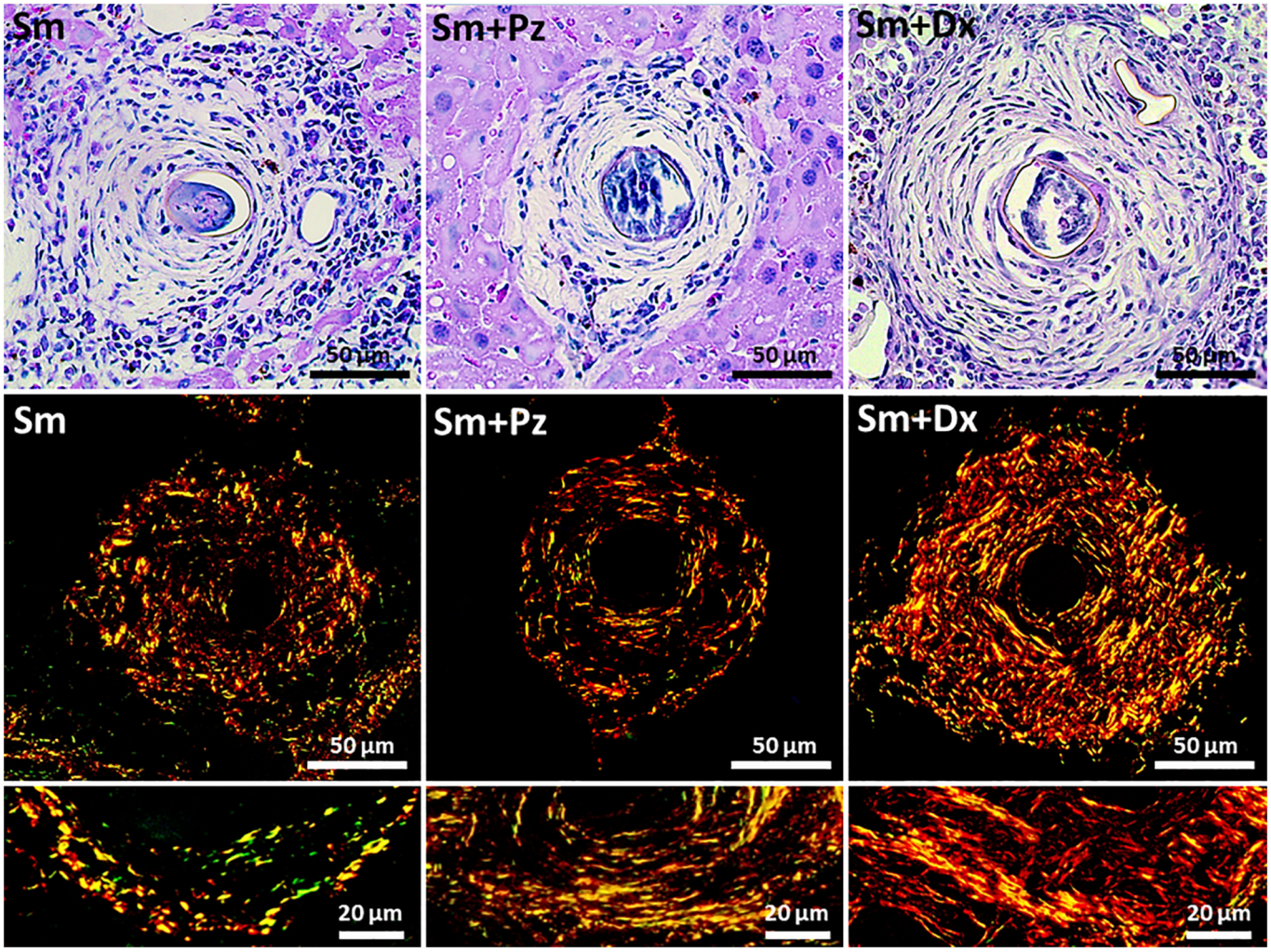

Fig. 12. Representative photomicrographs of hepatic granulomas in *Schistosoma mansoni*-infected mice untreated and treated with doxycycline (Dx) and praziquantel (Pz). Sm: infected with *S. mansoni*, Sm + Pz: infected with *S. mansoni* and treated with a single dose of Pz (200 mg/kg), Sm + Dx: infected with *S. mansoni* and treated for 60 days with Dx (50 mg/kg/day). Upper images (first line): staining with hematoxylin and eosin, light field microscopy. Lower images (second and third lines): Sirius red coloration, polarized light microscopy. (For interpretation of the references to color in this figure legend, the reader is referred to the web version of this article.)

infected animals. As Pz-treated animals showed a predominance of involutive granulomas, a high collagen accumulation was already expected [74,75]. However, intense fibrosis is not typical of exudative-productive granulomas, indicating that Dx may be involved in collagenogenesis modulation in the early stages of granuloma organization. As animals treated with Dx, but not with Pz, showed intense inhibition of the two MMPs with greater hepatic expression and activity (MMP-2 and MMP-9), the increase in collagen deposition may be related to the lower degradation rate of this molecule. Although hepatic fibrosis is often attributed to the intense activation of fibroblast and perisinusoidal cells by TGF-β in schistosomiasis [76–78], similar levels of this molecule do not explain the greater collagen accumulation in Dx-treated animals compared with untreated infected animals. Thus, our findings suggest that inhibition of MMPs activity may represent an important mechanism associated with hepatic fibrogenesis in response to Dx.

The imbalance between collagen synthesis and degradation is a common feature of schistosomiasis, culminating in hepatic fibrosis with slow and diffuse development, progressive vascular obstruction and portal hypertension [78,79]. As indicated by our findings, there is evidence that *S. mansoni*-induced granulomatous inflammation is accompanied by increased MMP activity, although this enzymatic reaction is unable to prevent hepatic fibrosis in chronic infections [15,79]. Vaillant et al. [80] observed a significant increase in expression of MMP-2, −3, −9, −12 and − 13 in *S. mansoni*-infected C57BL/6 mice. Sandler et al. [22] showed drastic induction of MMP-12 expression in liver and lung tissue in animals exposed to *S. mansoni* eggs, and Madala et al. [17] suggested that MMP-12 expression is related to the development of fibrosis from a Th2-dependent immune response. In addition to participating in granuloma remodeling throughout the infection, increased MMPs production and activity indicates a protective reaction that attenuates the progression of liver fibrosis [15,79]. As Dx exerts a potent inhibitory effect on MMP activity [81,82], our findings corroborate the hypothesis that this drug is potentially harmful to the host, modifying the collagen dynamics and granuloma organization in favor of hepatic fibrosis.

5. Conclusion

Our findings indicated that Dx induced a dose-dependent schistosomicidal effect *in vitro*. At concentrations even below the LD_{50} value, Dx induced morphological alterations in the *S. mansoni* integument similar to those caused by Pz. As the increase in severity of integumentary damage was accompanied by a higher rate of parasitic mortality, integument disorganization indicated a potential mechanism of Dx toxicity in *S. mansoni*. Even in the absence of significant

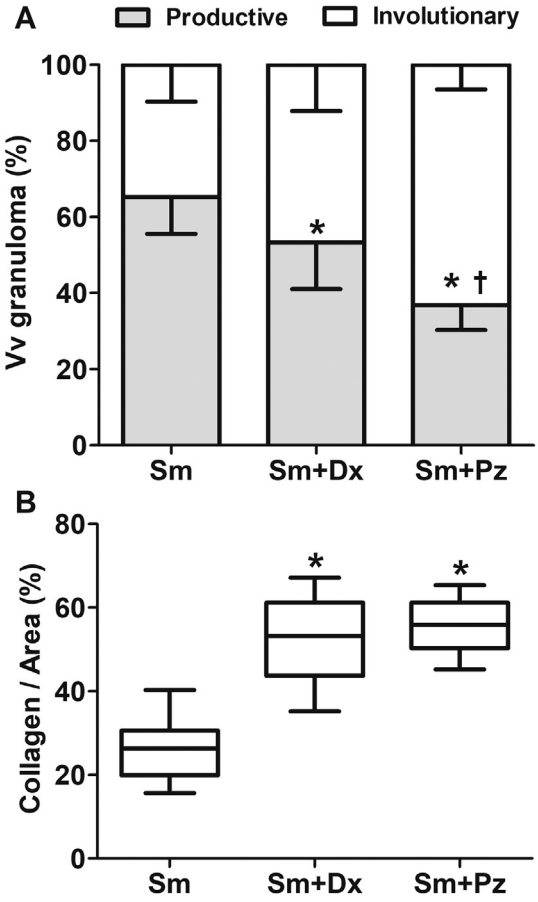

Fig. 13. Distribution of exudative-productive and involutive granulomas, and collagen content normalized by granuloma area in *Schistosoma mansoni*-infected mice untreated and treated with doxycycline (Dx) and praziquantel (Pz). Sm: infected with *S. mansoni*, Sm + Pz: infected with *S. mansoni* and treated with a single dose of Pz (200 mg/kg), Sm + Dx: infected with *S. mansoni* and treated for 60 days with Dx (50 mg/kg/day). The results are represented as median and interquartile range. Statistical difference ($P < 0.05$) in relation to the group *Sm and †Sm + Dx.

integumentary lesions, low doses of Dx impaired reproductive viability and induced some degree of parasitic mortality, indicating that the schistosomicidal effect of Dx may be more complex than an isolated action on the integument of adult *S. mansoni* worms. Contrary to its *in vitro* efficacy, Dx treatment was potentially harmful in *S. mansoni*-infected mice, aggravating granulomatous inflammation and pathological morphofunctional hepatic remodeling. Thus, this drug stimulated collagen deposition and modified the organization of hepatic granulomas, a process potentially related to the attenuation in collagenolysis mechanisms in response to MMP-2 and MMP-9 inhibition.

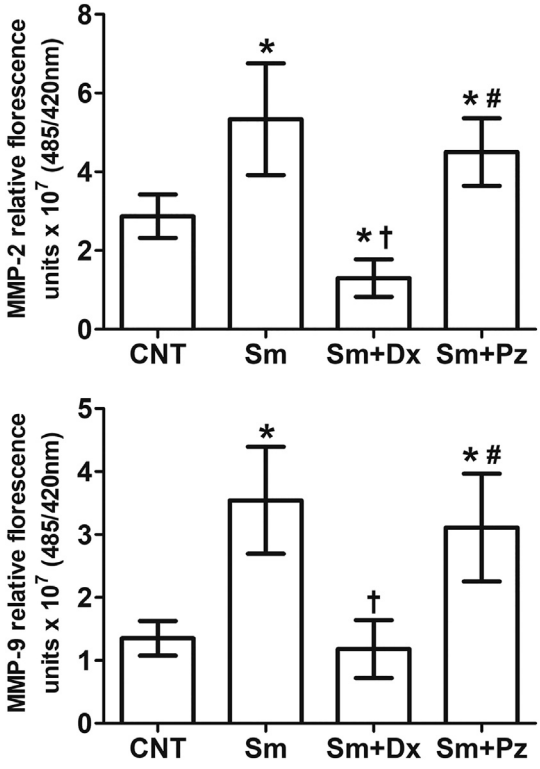

Fig. 14. Hepatic activity of metalloproteinases (MMPs) 2 and 9 in *Schistosoma mansoni*-infected mice untreated and treated with doxycycline (Dx) and praziquantel (Pz). CNT: uninfected control, Sm: infected with *S. mansoni*, Sm + Pz: infected with *S. mansoni* and treated with a single dose of Pz (200 mg/kg), Sm + Dx: infected with *S. mansoni* and treated for 60 days with Dx (50 mg/kg/day). The results are represented by mean and standard deviation. Statistical difference ($P < 0.05$) in relation to the group *CNT, †Sm, #Sm + Dx.

Acknowledgements

This work was supported by the Brazilian agencies: Fundação do Amparo à Pesquisa do Estado de Minas Gerais (FAPEMIG, processes APQ-01895-16 and PPM-00077-18) and Conselho Nacional de Desenvolvimento Científico e Tecnológico (CNPq, processes 303972/2017-3 and 423594/2018-4). This study was financed in part by the Coordenação de Aperfeiçoamento de Pessoal de Nível Superior - Brasil (CAPES) – Finance Code 001. We thank the Núcleo de Microscopia e Microanálise of the Federal University of Viçosa - UFV (Brazil) for assistance in electron microscopy.

References

[1] P.F. Basch, Schistosomes: Development, Reproduction, and Host Relations, Oxford University Press, New York, 1991, p. 264.
[2] D.G. Colley, et al., Human schistosomiasis, Lancet 383 (9936) (2014) 2253–2264.
[3] K.G.A.D. Weerakoon, G.N. Gobert, P. Cai, D. Mcmanus, Advances in the diagnosis of human schistosomiasis, Clin. Microbiol. Rev. 28 (4) (2015) 939–967.
[4] WHO, Department of control of neglected tropical diseases. Schistosomiasis and soil-transmitted helminthiases: number of people treated in 2016. Weekly Epidemiological Record, v. vol. 92, p. 749–760, 2017.
[5] E.V. De Melo, et al., A comparative cross-sectional study on the prevalence and morbidity of schistosomiasis in a community in northeastern Brazil (1979-2010), Mem. Inst. Oswaldo Cruz 109 (3) (2014) 340–344.
[6] D.V.B. Marques, A.A. Felizardo, R.L.M. Souza, A.A.C. Pereira, R.V. Gonçalves, R.D. Novaes, Could diet composition modulate pathological outcomes in schistosomiasis mansoni? A systematic review of in vivo preclinical evidence, Parasitology 145 (9) (2018) 1127–1136.
[7] J. Farrar, Manson's Tropical Infectious Diseases, 23 ed., Elsevier, New York, 2014.
[8] Milan, E.P; Keim, L. S. Esquistomíase Masônica Rotinas de diagnóstico e tratamento das doenças infecciosas e parasitárias. 2 ed. São Paulo: Atheneu; p. 345–50; 2007.
[9] C.H. King, Toward the elimination of schistosomiasis, N. Engl. J. Med. 360 (2) (2009) 106–109.
[10] Z.A. Andrade, *Schistosoma mansoni.* Esquistossomose uma visão multidisciplinar, A Patologia da Esquistossomose, Fiocruz, Rio de Janeiro, 2008.
[11] P. Raso, J. Neves, Contribuição ao conhecimento do quadro anatômico do fígado na forma toxêmica da esquistossomose mansônica através das punções-biopsias, Anais da Faculdade de Medicina de Minas Gerais 5 (1965) 147–165.
[12] K.B. Amaral, et al., Histological assessment of granulomas in natural and experimental *Schistosoma mansoni* infections using whole slide imaging, PLoS One 12 (9) (2017) 1–20.
[13] E. Hams, et al., The Schistosoma granuloma: friend or foe? Front. Immunol. 4 (89) (2013) 1–8.
[14] Z.A. Andrade, A. Prata, Asymptomatic schistosomiasis studied by needle biopsy of the liver, The American Journal of Tropical Medicine nd Hygiene 5 (1963) 236–242.
[15] D.E. Gomez, et al., Expression of metalloproteinases (MMP-1, MMP-2, and MMP-9) and their inhibitors (TIMP-1 and TIMP-2) in schistosomal portal fibrosis, Am. J. Trop. Med. Hyg. 61 (1) (1999) 9–13.
[16] S. Takahashi, M.A. Dunn, S. Seifter, Liver collagenase in murine schistosomiasis, Gastroenterology 78 (1980) 1425–1431.
[17] S.K. Madala, et al., Matrix metalloproteinase 12-deficiency augments extracellular

matrix degrading metalloproteinases and attenuates IL-13-dependent fibrosis, J. Immunol. 184 (7) (2010) 3955–3963.
[18] Y.P. Han, Matrix metalloproteinases, the pros and cons, in liver fibrosis, J. Gastroenterol. Hepatol. 21 (Suppl. 3) (2006) S88–S91.
[19] T.A. Wynn, Common and unique mechanisms regulate fibrosis in various fibroproliferative diseases, J. Clin. Investig. 117 (2007) 524–529.
[20] C.A. Tallant, Matrix metalloproteinases: fold and function of their catalytic domains, Biochim. Biophys. Acta 1803 (2010) 20–28.
[21] T. Sabo-Attwood, et al., Gene expression profiles reveal increased mClca3 (Gob5) expression and mucin production in a murine model of asbestos-induced fibrogenesis, Am. J. Pathol. 167 (2005) 1243–1256.
[22] N.G. Sandler, et al., Global gene expression profiles during acute pathogen-induced pulmonary inflammation reveal divergent roles for Th1 and Th2 responses in tissue repair, J. Immunol. 171 (2003) 3655–3667.
[23] S.L. Pender, et al., Role of macrophage metalloelastase in gut inflammation, Ann. N. Y. Acad. Sci. 1072 (2006) 386–388.
[24] T. Gaillard, et al., Tetracyclines in malaria, Malar. J. 14 (2015) 445.
[25] V. Rajendran, et al., Improved efficacy of doxycycline in liposomes against *Plasmodium falciparum* in culture and *Plasmodium berghei* infection in mice, Can. J. Physiol. Pharmacol. 3 (2018) 1–8.
[26] A. Horauf, et al., Doxycycline in the treatment of human onchocerciasis: kinetics of *Wolbachia endobacteria* reduction and of inhibition of embryogenesis in female Onchocerca worms, Microbes Infect. 5 (2003) 261–273.
[27] S.R. Smithers, R.J. Terry, The infection of laboratory hosts with cercariae of *Schistosoma mansoni* and the recovery of adults worms, Parasitology 55 (1965) 695–700.
[28] A.P. Castro, et al., Potent Schistosomicidal constituents from *Garcinia brasiliensis*, Planta Med. 81 (9) (2015) 733–741.
[29] P.L. Sequetto, et al., Naringin accelerates the regression of pre-neoplastic lesions and the colorectal structural reorganization in a murine model of chemical carcinogenesis, Food Chem. Toxicol. 64 (2014) 200–209.
[30] P.L. Sequetto, et al., Low doses of simvastatin potentiate the effect of sodium alendronate in inhibiting bone resorption and restore microstructural and mechanical bone properties in glucocorticoid-induced osteoporosis, Microsc. Microanal. 23 (5) (2017) 989–1001.
[31] S.N. El-Beshbishi, et al., Spotlight on the in vitro effect of artemisinin-naphthoquine phosphate on *Schistosoma mansoni* and its snail host *Biomphalaria alexandrina*, Acta Trop. 141 (2015) 37–45.
[32] A.L. Silva, et al., Tegumental changes in adult *Schistosoma mansoni* induced by a new imidazolidinic derivative, Br. J. Pharm. Res. 4 (16) (2014) 1988–2005.
[33] N. Araújo, et al., Oxamniquine, praziquantel and lovastatin association in the experimental *Schistosomiasis mansoni*, Mem. Inst. Oswaldo Cruz 103 (5) (2008) 450–454.
[34] G. De Paula Costa, et al., Doxycycline and benznidazole reduce the profile of Th1, Th2, and Th17 chemokines and chemokine receptors in cardiac tissue from chronic *Trypanosoma cruzi*-infected dogs, Mediat. Inflamm. 2016 (2016) 1–11.
[35] R.D. Novaes, et al., *Trypanosoma cruzi* infection and benznidazole therapy independently stimulate oxidative status and structural pathological remodeling of the liver tissue in mice, Parasitol. Res. 114 (8) (2015) 2873–2881.
[36] R.V. Gonçalves, et al., Hepatoprotective effect of Bathysa cuspidata in a murine model of severe toxic liver injury, Int. J. Exp. Pathol. 93 (2012) 370–376.
[37] E.C. Santos, et al., Concomitant benznidazole and suramin chemotherapy in mice infected with a virulent strain of Trypanosoma cruzi, Antimicrob. Agents Chemother. 59 (10) (2015) 5999–6006.
[38] Cardoso, L. M., Novaes, R.D., Castro, C.A., Novello, A.A., Goncalves, R.V., Ricci-Silva, M.E., Ramos, H.J.O., Peluzio, M.C.G., Leite, J.P.V. Chemical composition, characterization of anthocyanins and antioxidant potential of *Euterpe edulis* fruits: applicability on genetic dyslipidemia and hepatic steatosis in mice, Nutr. Hosp., v. 32, p. 702–709, 2015.
[39] L.C. Junqueira, L.M.M. Junqueira, Técnicas básicas de citologia e histologia, São Paulo: Santos (1983).
[40] R.D. Novaes, et al., *Trypanosoma cruzi* infection induces morphological reorganization of the myocardium parenchyma and stroma, and modifies the mechanical properties of atrial and ventricular cardiomyocytes in rats, Cardiovasc. Pathol. 22 (2013) 270–279.
[41] W. Garvey, et al., Combined modified periodic acid-Schiff and batch staining method, J. Histotechnol. 15 (2) (1992) 117–120.
[42] J.P.F. Rodrigues, et al., S. mansoni-T. cruzi co-infection modulates arginase-1/iNOS expression, liver and heart disease in mice, Nitric Oxide 66 (2017) 43–52.
[43] R.D. Novaes, et al., Effects of *Trypanosoma cruzi* infection on myocardium morphology, single cardiomyocyte contractile function and exercise tolerance in rats, Int. J. Exp. Pathol. 92 (2011) 299–307.
[44] M.C. Roberts, Tetracycline therapy: update, Clin. Infect. Dis. 36 (2003) 462–467.
[45] B. Sloan, N. Scheinfeld, The use and safety of doxycycline hyclate and other second-generation tetracyclines, Expert Opin. Drug Saf. 7 (2008) 571–577.
[46] D. Schnappinger, W. Hillen, Tetracyclines: antibiotic action, uptake, and resistance mechanisms, Arch. Microbiol. 165 (1996) 359–369.
[47] M.J. Taylor, et al., Macrofilaricidal activity after doxycycline treatment of *Wuchereria bancrofti*: a double-blind, randomized placebo-controlled trial, Lancet 365 (2005) 2116–2121.
[48] Santiago, E. deF. et al. Evaluation of the anti-*Schistosoma mansoni* activity of thiosemicarbazones and thiazoles. *Antimicrob. Agents Chemother.*, v. 58, n. 1, p. 352–363, 2014.
[49] G. Otunola, et al., Characterization, antibacterial and antioxidant properties of silver nanoparticles synthesized from aqueous extracts of *Allium sativum*, *Zingiber officinale*, and *Capsicum frutescens*, Pharmacognosy Journal 13 (50) (2017) S201–S208.
[50] L. Sanderson, A. Bartlett, P.J. Whitfield, In vitro and in vivo studies on the bioactivity of a ginger (*Zingiber officinale*) extract towards adult schistosomes and their egg production, J. Helminthol. 76 (3) (2002) 241–247.
[51] S. William, S. Botros, Validation of sensitivity to praziquantel using *Schistosoma mansoni* worm muscle tension and ca^{2+}-uptake as possible in vitro correlates to in vivo ED50 determination, Int. J. Parasitol. 34 (8) (2004) 971–977.
[52] F.G. Abath, R.C. Werkhauser, The tegument of *Schistosoma mansoni*: functional and immunological features, Parasite Immunol. 18 (1) (1996) 15–20.
[53] J.J. Van Hellemond, et al., Functions of the tegument of schistosomes: clues from the proteome and lipidome, Int. J. Parasitol. 36 (6) (2006) 691–699.
[54] X. Shuhua, et al., Tegumental changes in adult *Schistosoma mansoni* harboured in mice treated with praziquantel enantiomers, Acta Trop. 76 (2) (2000) 107–117.
[55] T. Manneck, Y. Haggenmüller, J. Keiser, Morphological effects and tegumental alterations induced by mefloquine on schistosomula and adult flukes of *Schistosoma mansoni*, Parasitology 137 (1) (2010) 85–98.
[56] S.H. Xiao, B.A. Catto, The profilatic effects of Artemether against *Schistosoma japonicum* infections, Parasitol. Today 16 (2000) 122–126.
[57] Rey, L. Parasitologia.In: *Schistosoma mansoni* e esquistossomose: a doença, Rio de Janeiro, p. 413–443, 2001.
[58] M.H. Kaplan, Th2 cells are required for the *Schistosoma mansoni* egg-induced granulomatous response, J. Immunol. 160 (1998) 1850–1856.
[59] O.M. Abdallahi, S. Hanna, M. De Reggi, B. Gharib, Visualization of oxygen radical production in mouse liver in response to infection with *Schistosoma mansoni*, Munksgaard 19 (1999) 495–500.
[60] A.C. La Flamme, et al., IL-4 plays a crucial role in regulating oxidative damage in the liver during *Schistosomiasis*, J. Immunol. 166 (2001) 1903–1911.
[61] H. Cichoż-Lach, A. Michalak, Oxidative stress as a crucial factor in liver diseases, World J. Gastroenterol. 20 (25) (2014) 8082–8091.
[62] T. Mello, et al., Oxidative stress in the healthy and wounded hepatocyte: a cellular organelles perspective, Oxidative Med. Cell. Longev. (2016) 1–15.
[63] C. Guillot, et al., Lethal hepatitis after gene transfer of IL-4 in the liver is independent of immune responses and dependent on apoptosis of hepatocytes: a rodent model of IL-4-induced hepatitis, J. Immunol. 166 (2001) 5225–5235.
[64] L. Yang, et al., TGF-β signaling in hepatocytes participates in steatohepatitis through regulation of cell death and lipid metabolism, Hepatology 59 (2) (2014) 483–495.
[65] G. Schramm, H. Haas, Th2 immune response against *Schistosoma mansoni* infection, Microbes Infect. 12 (2010) 881–888.
[66] L. Aoudjehane, et al., Interleukin-4 induces human hepatocyte apoptosis through a Fas-independent pathway, FASEB J. 21 (2007) 1433–1444.
[67] H.F. Löhr, et al., Phenotypical analysis and cytokine release of liver-infiltrating and peripheral blood T lymphocytes from patients with chronic hepatitis of different etiology, Liver 14 (1994) 161–166.
[68] O.M. Martinez, et al., Cytokine patterns and cytotoxic mediators in primary biliary cirrhosis, Hepatology 21 (1) (1995) 113–119.
[69] S. Franckhauser, et al., Overexpression of IL 6 leads to hyperinsulinaemia, liver inflammation and reduced body weight in mice, Diabetologia 51 (2008) 1306–1316.
[70] B.M. Melgert, et al., Targeting dexamethasone to Kupffer cells: effects on liver inflammation and fibrosis in rats, Hepatology 34 (4) (2001) 719–727.
[71] F. Götschel, et al., Inhibition of GSK3 differentially modulates NF-κB, CREB, AP-1 and β-catenin signaling in hepatocytes, but fails to promote TNF-α-induced apoptosis, Experimental Cell Reserch 314 (2008) 1351–1366.
[72] M. Martin, et al., Toll-like receptor-mediated cytokine production is differentially regulated by glycogen synthase kinase 3, Nat. Immunol. 6 (8) (2005) 777–784.
[73] S. Bassily, et al., Praziquantel for treatment of schistosomiasis in patients with advanced hepatosplenomegaly, Ann. Trop. Med. Parasitol. 79 (6) (15 January 1985) 629–634.
[74] Z.A. Andrade, Schistosomiasis and liver fibrosis, Parasite Immunol. 31 (2009) 656–663.
[75] A.A. Badawy, et al., Evaluation of colchicine with or without praziquantel therapy in the control of hepatic fibrosis in murine schistosomiasis, Pharmacol. Res. 33 (6) (1996) 319–325.
[76] A.R. De Jesus, et al., Association of Type 2 cytokines with hepatic fibrosis in human *Schistosoma mansoni* infection, Infect. Immun. 72 (2004) 3391–3397.
[77] I.O. Farah, et al., Repeated exposure induces periportal fibrosis in *Schistosoma mansoni*-infected baboons: role of TGF- b and IL-4, J. Immunol. 164 (2000) 5337–5343.
[78] T.A. Wynn, Fibrotic disease and the Th1/Th2 paradigm, Nature Reviews 4 (2004) 583–594.
[79] K.P. Singh, Expression of matrix metalloproteinases and their inhibitors during the resorption of schistosome egg-induced fibrosis in praziquantel-treated mice, Immunology 111 (2004) 343–352.
[80] B. Vaillant, et al., Regulation of hepatic fibrosis and extracellular matrix genes by the Th response: new insight into the role of tissue inhibitors of matrix metalloproteinases, J. Immunol. 167 (2001) 7017–7026.
[81] M.M. Castro, et al., Matrix metalloproteinase inhibitor properties of tetracyclines: therapeutic potential in cardiovascular diseases, Pharmacol. Res. 64 (2011) 551–560.
[82] J.T. Peterson, Matrix metalloproteinase inhibitor development and the remodeling of drug discovery, Heart Fail. Rev. 9 (2004) 63–79.
[83] D. Katiyar, L.K. Singh, Filariasis: current status, treatment and recent advances in drug development, Curr. Med. Chem. 18 (14) (2011) 2174–2185.
[84] M.J. Taylor, A. Hoerauf, S. Townson, B.E. Slatko, S.A. Ward, Anti-Wolbachia drug discovery and development: safe macrofilaricides for onchocerciasis and lymphatic filariasis, Parasitology 141 (1) (2014) 119–127.
[85] A.M. Mohamed, N.M. Metwally, S.S. Mahmoud, Sativa seeds against Schistosoma mansonidifferent stages, Mem. Inst. Oswaldo. Cruz. 100 (2) (2005) 205–211.
[86] S. William, S. Botros, M. Ismail, A. Farghally, Praziquantel-induced tegumental damage in vitro is diminished in schistosomes derived from praziquantel-resistant infections, Parasitology 122 (1) (2001) 63–66.